The International Archives of the Photogrammetry, Remote Sensing and Spatial Information Sciences, Volume XLVIII-M-6-2025
ISPRS, EARSeL & DGPF Joint Istanbul Workshop "Topographic Mapping from Space" dedicated to Dr. Karsten Jacobsen's 80th Birthday
29–31 January 2025, Istanbul, Türkiye

A Review on Geo3o1 for 3D Georeferencing Accuracy Assessment of State-of-the-Art Sensor Dependent Orientation Model

Hüseyin Topan

Dept. of Geomatics Engineering, Faculty of Engineering, Zonguldak Bülent Ecevit University, 67100 Zonguldak, Türkiye – topan@beun.edu.tr

Keywords: block adjustment by conditions, georeferencing accuracy, sensor-dependent orientation, Pléiades 1A.

Abstract

Geo3o1 is a Matlab tool for 3D georeferencing accuracy retrieval for Pléiades 1A/1B/Neo, SPOT 6/7 and Göktürk-1 stereo or triplet primary panchromatic images. Even though the orientation model was settled by the image providers, the main contribution of Geo3o1 is the two-stage adjustment computation. Moreover, exterior orientation parameters' efficiency and validation, and also the correlation between interior and exterior orientation parameters could be analysed. Geo3o1 is capable of processing stereo or triplet images. The case study was handled with the panchromatic primary triplet images of Pléiades 1A. 171 points measured by GNSS observations were used. The accuracy on the ground was estimated at the centimetre level for GCPs, while the accuracy for ICPs was naturally coarser at ~ ± 1 GSD in bundle adjustment. The external orientation parameters' effectiveness and validation, and co- and cross-correlations were also investigated. The test site covers a hilly, mountainous area in Zonguldak, Türkiye.

1. Introduction

1.1 Georeferencing of Remote Sensing Images

Georeferencing of remote sensing images is a key process to generate the geospatial information. This process needs the coordinate transformation between image and ground. Although the collinearity equations, or its derivation such as DLT (Direct Linear Transformation) developed by Abdel-Aziz and Karara (1971), the linear array imaging geometry and satellite's dynamic movement in its orbit during the imaging need those approaches' adoption.

Although some merits were recorded before SPOT-1, the first satellite of the French Space Agency's long term, the focus on geospatial information retrieval were started with its launch in 1986. SPOT series continued with its 6th and 7th sisters, and Pléiades 1A, 1B and Neo in operation. The importance of this satellite is that the collinearity equations were adopted to its linear array imaging geometry (Konecny et al., 1987; Toutin, 1983). This mission were subjected by many researchers as listed by Topan (2009), and Topan and Maktav (2014).

2000s witnessed many developments in image based geospatial information generation both in photogrammetry and remote sensing. While the digital photogrammetric cameras and laser scanners were the major development in terrestrial and aerial photogrammetry, the IKONOS satellite started a new area in remote sensing thanks to its sub-pixel GSD (Ground Sampling Distance) following its launch in 1999. The RFM (Rational Functional Model) became the generic sensor orientation model instead of the collinearity based approaches (i.e. sensor dependent orientation model). The advantage of RFM was that the formulation was constant, and the RPCs (Rational Functional Models) were given by the image vendors for each images, or the user can estimate them using accurate and dense GCPs (Ground Control Points).

Although the RFM was settled as generic georeferencing model by OGC (1999), the sensor depending orientation models based on the collinearity equations are still being needed. The requirement might be caused by the motivations i) 2/3 dimensional direct georeferencing of images without GCPs, ii) estimating the RPCs in mono or stereo modes, iii) assessing the accuracy of interior and exterior parameters, and so iv) designing the new equipment for future missions. The most useful outcome for the end-users might be the estimating the RPCs in two types, i.e. from ground to image and vice versa. The recent research on the sensor dependent orientation models subjected the Chinese satellites. Before detailed reviewing of Geo3o1, GeoSpot, the tool developed for SPOT-5 stereo images, and related works must be revisited.

1.2 GeoSpot

Only two researchers in Türkiye, Orun and Natarajan, focused on developing a parametric model (Orun, 1990; Orun and Natarajan, 1994) whereas many researchers have their own sensor dependent orientation models in overseas. Following the author's master science thesis under the supervision of Prof. Gürcan Büyüksalih and the contribution of Dr.-Ing. Karsten Jacobsen in the Department of Geomatics Engineering in Zonguldak Bülent Ecevit (formerly Zonguldak Karaelmas) University, evaluating the IRS-1C panchromatic image (Topan, 2004), the author decided to focus on the sensor dependent orientation models. This was available with studying the SPOT 5 HRG level 1A stere panchromatic images which were already available for the research group (Büyüksalih et al., 2005). As a doctor of philosophy thesis, the author developed the GeoSpot as a tool of (GeoEtrim, 2025; Topan, 2009). GeoSpot did not aim to develop a new model, i.e. the model was modified by Riazanoff (2004) from the generic form which was explained in detail by Weser et al. (2007) and Weser et al. (2008). Fotev et al. (2005) simplified the rotation matrix between payload and orbit to remove the trigonometric functions. GeoSpot suggested a two-step adjustment approach to mitigate the effect of interior orientation represented by the look angles. The results showed that the look angles were the major error source for georeferencing accuracy, and EOPs (Exterior Orientation Parameter) could be kept with their initial values. GeoSpot can estimate the validation of EOPs, and also the correlation between interior and exterior orientation parameters (Topan, 2009; Topan and Maktav, 2014). The codes of GeoSpot are open in GitHub repository (GeoEtrim, 2025).
Although GeoSpot was successfully applied for estimating georeferencing accuracy in 3D for SPOT-5 HRG level 1A stereo images, it must have been handled with respect to the ill posed problem. Various EOP sets could be chosen in the adjustment, nevertheless some of them resulted unrealistic inaccurate results. Terlemezoğlu and Topan (2020) proposed a novel approach choosing a proper eigenvalue of normal equation, and showed the usability of Moore-Penrose inversion, not only for the GeoSpot, but also for the GeoTransform, the tool for sensor independent orientation models.

1.3 Geo3o1

Developing a tool for sensor dependent orientation model of was one of the aims of the Pléiades-1A projects (Topan et al., 2016). However, the difference between the sensor dependent orientation models of SPOT-5 and Pléiades 1A, and the necessary of programming improvements forced to start a new tool called Geo3o1 (3 refers the triplet imaging mode and 1 refers the one pass). The remainder of this paper presents the formulation of Geo3o1, the images, test site, and ground truth data, and the results. Finally, the further studies will be presented in the concluding remarks.

2. Mathematical Background

Although the principal formulation of the orientation model is same, some minor differences are available for SPOT 1-5 and for Pléiades-1A/1B/Neo, SPOT 6/7 and Göktürk-1. Firstly, the level of image products is different. Level 1A for SPOT 1-5 kept the original geometry although the radiometrically processed. The basic level is defined as *primary* for Pléiades-1A/1B/Neo, *sensor* for SPOT 6&7, and *level 2A* for Göktürk-1. The new image product levels (primary, sensor or level 2A) illustrates a virtual image combining the multiple linear arrays (Airbus Defence and Space, 2012, 2013, 2022). Secondly, the looking angles were given for each column of the image while they are given as the coefficients of 2nd order polynomial in the newer version. Third modification is that the orientation from payload to ground was estimated step by step while it is done by quaternion coefficients with 3rd order polynomial in one-step.

According to Airbus Defence and Space (2012, 2013, 2022), image to ground transformation is following,

$$\vec{\boldsymbol{P}}_{\boldsymbol{i}} = \begin{bmatrix} \mathrm{X}_i \\ \mathrm{Y}_i \\ \mathrm{Z}_i \end{bmatrix} = \vec{\boldsymbol{P}}_{\boldsymbol{S}_i} - m_i \, \underline{\boldsymbol{R}}_i \begin{bmatrix} -\tan\psi_{y_i} \\ \tan\psi_{x_i} \\ -1 \end{bmatrix} \tag{1}$$

where $\vec{\boldsymbol{P}}_{\boldsymbol{i}} = [\mathrm{X}_i \quad \mathrm{Y}_i \quad \mathrm{Z}_i]^{\mathrm{T}}$ is the position vector in Cartesian coordinate system for object, $\vec{\boldsymbol{P}}_{\boldsymbol{S}_{\boldsymbol{i}}}$ is the position vector of satellite's mass center in Cartesian coordinate system, m defines scale, $\underline{\boldsymbol{R}}_i$ is the rotation matrix by normalized quaternions, (ψ_{x_i}, ψ_{y_i}) shows look angles, and i denotes the running index for the point i. Below is the rotation matrix $\underline{\boldsymbol{R}}$ expressed in quaternions.

$$\begin{aligned}
r_{11} &= (Q_0^n)^2 + (Q_1^n)^2 - (Q_2^n)^2 - (Q_3^n)^2 \\
r_{12} &= 2(Q_1^n Q_2^n - Q_0^n Q_3^n) \\
r_{13} &= 2(Q_1^n Q_3^n + Q_0^n Q_2^n) \\
r_{21} &= 2(Q_1^n Q_2^n + Q_0^n Q_3^n) \\
r_{22} &= (Q_0^n)^2 - (Q_1^n)^2 + (Q_2^n)^2 - (Q_3^n)^2 \\
r_{23} &= 2(Q_2^n Q_3^n - Q_0^n Q_1^n) \\
r_{31} &= 2(Q_1^n Q_3^n - Q_0^n Q_2^n) \\
r_{32} &= 2(Q_2^n Q_3^n - Q_0^n Q_1^n) \\
r_{33} &= (Q_0^n)^2 - (Q_1^n)^2 - (Q_2^n)^2 + (Q_3^n)^2
\end{aligned} \tag{2}$$

where normalised quaternions estimated by

$$Q_{j_i}^n = \frac{Q_{j_i}}{\sqrt{\underline{Q}_i^{\mathrm{T}} \underline{Q}_i}}, j = 0,1,2,3, \underline{Q}_i = \left[Q_{0_i} \; Q_{1_i} \; Q_{2_i} \; Q_{3_i}\right]^{\mathrm{T}}, \tag{3}$$

$$Q_{j_i} = \sum_{b=0}^{3} (Q_j)_b \, t_{\mathrm{CN}_i}^b \tag{4}$$

for Pléiades 1A/1B and Göktürk 1, while they are formulated for SPOT 6/7 and Pléiades Neo as following

$$\begin{aligned}
&Q_{j_i}^{\mathrm{n}} = Q_j^{\mathrm{n}}(t_k) + (Q_j^{\mathrm{n}}(t_{k+1}) - Q_j^{\mathrm{n}}(t_k)) \frac{t_i - t_k}{t_{k+1} - t_k} \\
&t_k < t_i < t_{k+1}, j = 0,1,2,3
\end{aligned} \tag{5}$$

$$Q_{j_i}^{\mathrm{n}} = Q_{j_0}^{\mathrm{n}} + \dot{Q}_j^{\mathrm{n}}(x_i - x_{\mathrm{ref}}) + \ddot{Q}_j^{\mathrm{n}}(x_i - x_{\mathrm{ref}})^2 \tag{6}$$

The centred normalized time value (t_{CN_i}) is calculated as

$$t_{\mathrm{CN}_i} = \frac{t_i - t_{\mathrm{offset}}}{t_{\mathrm{scale}}} \tag{7}$$

$$t_i = t_{\mathrm{ref}} + t_{\mathrm{period}}(x_i - x_{\mathrm{ref}}) \tag{8}$$

where t_i is the imaging time of i^{th} image line. t_k is the time stamp of corresponding Q_j^{n}, Q_{j_0} means quaternion for reference line, $\dot{Q}_j$ is quaternion's drift, and $\ddot{Q}_j$ is quaternion's drift rate.

The vector formed by the look angles is calculated by

$$\tan\psi_{y_i} = \sum_{b=0}^{n} (\psi_y)_b (y_i - y_{\mathrm{ref}}) \tag{9}$$

$$\tan\psi_{x_i} = \sum_{b=0}^{n} (\psi_x)_b (y_i - y_{\mathrm{ref}}) \tag{10}$$

where x and y are the row and column coordinates in image space, respectively.

The reverse form of Eq. (1), i.e. from ground to image, can be chosen in adjustment process as following

$$\begin{aligned}
\mathrm{F}_{\psi_{y_i}} &= \frac{R_{11_i}^{\mathrm{T}}(X_{s_i} - X_i) + R_{12_i}^{\mathrm{T}}(Y_{s_i} - Y_i) + R_{13_i}^{\mathrm{T}}(Z_{s_i} - Z_i)}{R_{31_i}^{\mathrm{T}}(X_{s_i} - X_i) + R_{32_i}^{\mathrm{T}}(Y_{s_i} - Y_i) + R_{33_i}^{\mathrm{T}}(Z_{s_i} - Z_i)} \\
&\quad - \tan\left(\psi_{y_i}\right) = 0 \\
\mathrm{F}_{x_i} &= \frac{R_{21_i}^{\mathrm{T}}(X_{s_i} - X_i) + R_{22_i}^{\mathrm{T}}(Y_{s_i} - Y_i) + R_{23_i}^{\mathrm{T}}(Z_{s_i} - Z_i)}{R_{31_i}^{\mathrm{T}}(X_{s_i} - X_i) + R_{32_i}^{\mathrm{T}}(Y_{s_i} - Y_i) + R_{33_i}^{\mathrm{T}}(Z_{s_i} - Z_i)} \\
&\quad - \tan\left(\psi_{x_i}\right) = 0
\end{aligned} \tag{11}$$

where $\underline{\boldsymbol{R}}^{-1} = \underline{\boldsymbol{R}}^{\mathrm{T}}$ since $\underline{R}$ is an orthogonal matrix.

$$\mathrm{X}_{S_i} = \mathrm{X}_{S_0} + \dot{\mathrm{X}}_S(x_i - x_{ref}) + \ddot{\mathrm{X}}_S(x_i - x_{ref})^2 \tag{12}$$

and is valid for Y_s and Z_s. $\vec{\boldsymbol{P}}_{\boldsymbol{S}}$ and its acquisition times, $(Q_j)_i$, t_{offset}, t_{ref}, t_{period}, t_{scale}, x_{ref}, y_{ref}, $\tan(\psi_y)_i$, $\tan(\psi_x)_i$ are directly taken from the Pléiades 1A/1B and Göktürk-1 metadata file while the normalised quaternions and their acquisition times are available from the metadata file of SPOT 6/7 and Pléiades Neo. In the functional model, the look angles (ψ_x, ψ_y) are considered observations. t_{offset}, t_{ref}, t_{period}, t_{scale}, coefficients of second order polynomial model for $\vec{\boldsymbol{P}}_{\boldsymbol{S}}$, coefficients of quaternions in case of Pléiades 1A/1B and Göktürk-1, and coefficients of normalised quaternions in case of SPOT 6/7 and Pléiades Neo, and approximate coordinates $(X, \; Y, \; Z)$ of check points (ICPs) are assumed parameters to be corrected. The user can choose one or a set of combination of them as adjustment parameters.

The functional model of adjustment by conditions is,

$$\underline{\boldsymbol{A}}\,\underline{\mathrm{dP}} + \underline{\boldsymbol{B}}\,\underline{\mathbf{v}} + \underline{w} = \underline{0} \tag{13}$$

where $\underline{A}$ and $\underline{B}$ denotes the Jacobian matrixes constituted by the EOP and observations (look angles), respectively, and $\underline{w}$ is the miscloser vector. The unknowns ($\underline{dP}$) are estimated as

$$\underline{\mathrm{dP}} = (\underline{\boldsymbol{A}}^{\mathrm{T}}(\underline{\boldsymbol{B}\boldsymbol{B}}^{\mathrm{T}})^{-1}\underline{\boldsymbol{A}} + \kappa\underline{\boldsymbol{E}})^{-1}\underline{\boldsymbol{A}}^{\mathrm{T}}(\underline{\boldsymbol{B}\boldsymbol{B}}^{\mathrm{T}})^{-1}\,\underline{w} \tag{14}$$

where κ is the one of proper eigenvalue of $\underline{\boldsymbol{A}}^{\mathrm{T}}\underline{\boldsymbol{A}}$ chosen as Tikhonov coefficient, and $\underline{\boldsymbol{E}}$ is the elementary matrix. The residuals are estimated as

$$\underline{\mathbf{v}} = \underline{\boldsymbol{B}}^{\mathrm{T}}\left(\underline{\boldsymbol{B}\boldsymbol{B}}^{\mathrm{T}}\right)^{-1}(\underline{\boldsymbol{A}}\underline{\mathrm{dP}} + \underline{w}) \tag{15}$$

Following the estimation of adjusted observation

$$\bar{\underline{\mathbf{L}}} = \underline{\boldsymbol{L}} + \underline{\mathbf{v}} \tag{16}$$

and adjusted parameters

$$\bar{\underline{\boldsymbol{P}}} = \underline{P}\big|_0 + \underline{\mathrm{dp}} \tag{17}$$

The condition $\mathrm{F}(\bar{\underline{\mathrm{P}}}, \bar{\underline{\mathrm{L}}}) \stackrel{?}{=} 0$ must be confirmed.

The $\underline{\boldsymbol{P}}$ are

$$\underline{\boldsymbol{P}} = \begin{bmatrix} t_{ref}\ t_{period}\ t_{offset}\ t_{scale} \dots \\ X_{S_0}\ \dot{X}_S\ \ddot{X}_S\ Y_{S_0}\ \dot{Y}_S\ \ddot{Y}_S\ Z_{S_0}\ \dot{Z}_S\ \ddot{Z}_S \dots \\ Q_{0_0}\ \dot{Q}_0\ \ddot{Q}_0\ \dddot{Q}_0\ Q_{1_0}\ \dot{Q}_1\ \ddot{Q}_1\ \dddot{Q}_1\ \dots \\ Q_{2_0}\ \dot{Q}_2\ \ddot{Q}_2\ \dddot{Q}_2\ Q_{3_0}\ \dot{Q}_3\ \ddot{Q}_3\ \dddot{Q}_3\ \dots \\ X_{ICP}\ Y_{ICP}\ Z_{ICP} \end{bmatrix}^{\mathrm{T}} \tag{18}$$

for Pléiades 1A/1B and Göktürk 1, and

$$\underline{\boldsymbol{P}} = \begin{bmatrix} X_{s_0}, \dot{X}_s, \ddot{X}_s, Y_{s_0}, \dot{Y}_s, \ddot{Y}_s, Z_{s_0}, \dot{Z}_s, \ddot{Z}_s \dots \\ Q^n_{0_0}, \dot{Q}^n_0, \ddot{Q}^n_0, Q^n_{1_0}, \dot{Q}^n_1, \ddot{Q}^n_1 \dots \\ Q^n_{2_0}, \dot{Q}^n_2, \ddot{Q}^n_2, Q^n_{3_0}, \dot{Q}^n_3, \ddot{Q}^n_3 \end{bmatrix}^{\mathrm{T}} \tag{19}$$

for SPOT 6/7 and Pléiades Neo.

The EOPs ($\underline{P}$) are assumed constant, and only the look angles $\underline{L}$ of ground control points (GCPs) are adjusted in the pre-adjustment step. In other words, $\underline{\mathrm{dP}} = 0 \rightarrow \underline{\boldsymbol{A}}\,\underline{\mathrm{dP}} = \underline{0}$, and the functional model becomes $\underline{\boldsymbol{B}}\,\underline{\mathbf{v}} + \underline{w} = \underline{0}$. The look angles of ICPs are interpolated using these pre-adjusted look angles of GCPs as following:

$$\boldsymbol{A}_{\psi_i} = [1\ (x - x_{\mathrm{ref}})_i\ (y - y_{\mathrm{ref}})_i], \psi \in (\psi_x, \psi_y) \tag{20}$$

$$b_{\psi_i} = [\psi_i] \tag{21}$$

$$\underline{c}_\psi = (\underline{\boldsymbol{A}}^{\mathrm{T}}_\psi\underline{\boldsymbol{A}}_\psi)^{-1}\underline{\boldsymbol{A}}^{\mathrm{T}}_\psi\underline{b}_\psi \tag{22}$$

$$\psi_{ICP} = \underline{c}^{\mathrm{T}}_\psi[1\ (x - x_{ref})_{ICP}\ (y - y_{ref})_{ICP}]^{\mathrm{T}} \tag{23}$$

The functional model of bundle adjustment is the expanded form of Eq. (13) consisting of numerous images. So, the difference between estimated coordinates (using adjusted look angles and EOPs) by the bundle adjustment and measured coordinates (by field survey) are the accuracy as following:

$$m_X = \pm\sqrt{\frac{[\Delta X \Delta X]}{p}}, m_Y = \pm\sqrt{\frac{[\Delta Y \Delta Y]}{p}}, m_Z = \pm\sqrt{\frac{[\Delta Z \Delta Z]}{p}} \tag{24}$$

where $\Delta X = \overline{\mathrm{X}}_{\mathrm{estimated}} - \mathrm{X}_{\mathrm{meausured}}$, and p is the number of GCP/ICPs.

In sensor dependent orientation, correlation among the EOPs and between EOPs and IOPs should be investigated. In this case the correlation is formulated as following:

$$\underline{Q}_{dpdp} = (\underline{\boldsymbol{A}}^{\mathrm{T}}(\underline{\boldsymbol{B}\boldsymbol{B}}^{\mathrm{T}})^{-1}\underline{\boldsymbol{A}})^{\mathrm{T}} \tag{25}$$

$$r_{dP_1 dP_2} = \frac{q_{dP_1 dP_2}}{\sqrt{q_{dP_1 dP_2} q_{dP_1 dP_2}}} \tag{26}$$

where $\underline{Q}_{dpdp}$ denotes auto-cofactor matrix consisting of $q_{dP_1 dP_2}$, and $r_{dP_1 dP_2}$ is the correlation among two unknowns of parameters P_1 and P_2. The possible correlation among the IOPs and EOPs can be estimated as following:

$$\underline{Q}_{\psi dp} = -\underline{\boldsymbol{B}^{\boldsymbol{T}}}\left(\underline{\boldsymbol{B}\boldsymbol{B}^{\boldsymbol{T}}}\right)^{-1}\underline{\boldsymbol{A}}\,\underline{\boldsymbol{A}^{\boldsymbol{T}}}(\underline{\boldsymbol{B}\boldsymbol{B}^{\boldsymbol{T}}})^{-1}\,\underline{\boldsymbol{A}} \tag{27}$$

$$r_{\psi dp} = \frac{q_{\psi dp}}{\sqrt{q_{\psi dp}}} \tag{28}$$

where $\underline{Q}_{\psi dp}$ is cross-cofactor matrix, and $r_{\psi dp}$ is the correlation among observations (IOPs) and unknowns (EOPs). Statistical validation of the parameters is also analysed as following.

$$m_0 = \pm\sqrt{\frac{\boldsymbol{\nu}\boldsymbol{\nu}^{\mathbf{T}}}{n-u}} \tag{29}$$

$$\mathrm{T} = \frac{|P_j|}{m_{dP_1}} \tag{30}$$

where m_0 and m_{dP_1} are root mean square error of unit weight and of parameters, respectively, and t is test value which must be greater than $t_{\alpha/2,f}$ for a valid parameter, where $\frac{\alpha}{2} = 0.025$ and $f = n - u$ is degree of freedom. Figure 1 illustrates the workflow of Geo3o1.

3. Images, Test Site and Ground Truth

This section presents the findings for the panchromatic images of Pléiades 1A tri-stereo primary product 50 cm GSD, dated 24th April 2013. The specifications and imaging configuration of the investigated images are presented in Table 1 and in Figure 2.a. The images covered the city centre of Zonguldak and its surroundings (Türkiye), a very suitable area for the study of remote sensing imagery, with its characteristics of undulating and varied land cover. Zonguldak city centre is also founded in this area along the Black Sea. The maximum height is 925 m for the imaged area. The field survey was held by the GNSS (Global Navigation Satellite Systems) observations in real time kinematic mode guarantying the 3D accuracy between ±4 mm to ±283 mm, and most were under the accuracy limit suggested by Kapnias et al. (2008). The symmetric objects were chosen on the bare ground as the points, horizontally and vertically evenly distributed. Figure 2.b presents the point distribution.

Stereopair	Δt (sec)	Base (km)	B/H	Convergence angle
283-284	20.75	156.7	0.22	12.8°
283-269	10.50	79.8	0.11	6.5°
269-284	10.25	76.9	0.11	6.3°

Table 1. Specifications of imaging configurations.

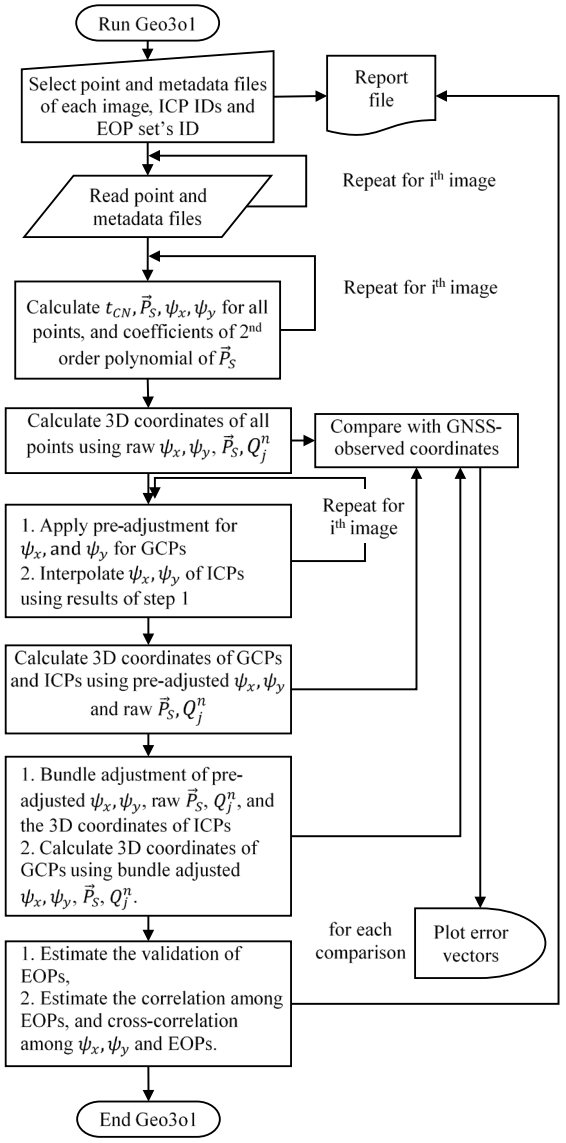

Figure 1. Workflow of Geo3o1.

4. Results

The results are presented with respect to the direct georeferencing, adjustment, and the validation and correlation tests.

4.1 Accuracy by Direct Georeferencing

Initial EOPs and look angles were used to estimate the direct georeferencing accuracy. The results presented in Table 2 confirm the accuracy expected ~8.5 m CE90 (circular error) at nadir viewing (Airbus Defence and Space, 2012). The stereopair with highest B/H and tri-stereo imaging did not bring an advantage for direct georeferencing accuracy. Figure 3 presents the vector plot for the stereopair with longest base.

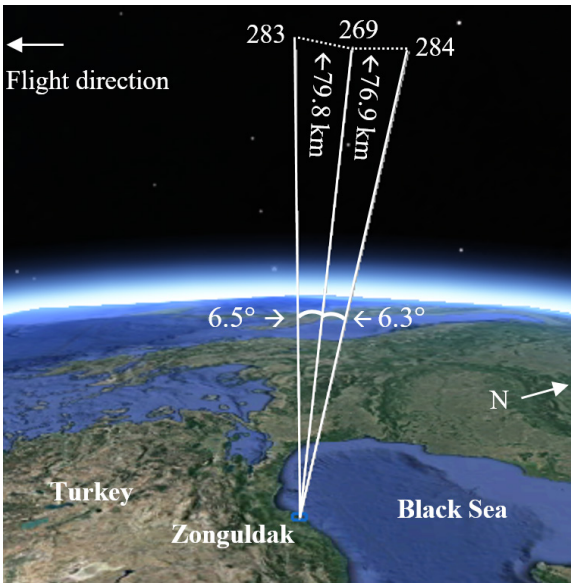

a) Imaging configuration (background image from Google Earth)

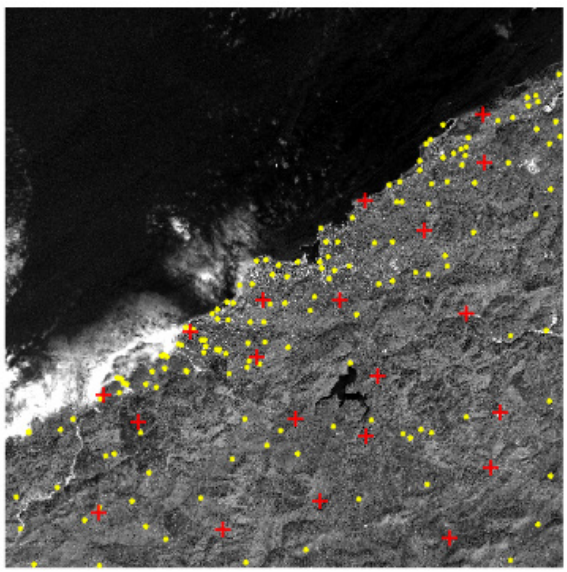

b) Point distribution (+: GCP, ◊: ICP)

Figure 2. Imaging configuration and point distribution.

Stereopair ID	m_x	m_y	m_z	m_{3D}
269-284	2.15	8.42	3.52	9.38
283-269	3.17	7.61	2.37	8.58
283-284	2.39	8.02	2.59	8.76
Triplet	2.43	8.00	2.64	8.77

Table 2. Results of 3D direct georeferencing accuracy (±m).

4.2 Accuracy, Validation and Correlation by Adjustment

The major outcome with the adjustment process is that bundle adjustment did not contribute the results following the pre-adjustment (Table 3). This means, the adjusting look angles was the key factor to reach the high accuracy. Various kinds of EOPs could be chosen in the bundle adjustment. The bundle adjustment results in Table 3 were generated by the EOP t_{ref}. All accuracies for GCPs were estimated under millimetre and about centimetre level after pre- and bundle adjustment applied, respectively, while the accuracies for ICPs were almost ~±1 GSD for all stereopairs except 269-284. Such kind of high accuracy at GCPs could be expected by adjustment as experienced by Leprince et al. (2007), Leprince et al. (2008) and Topan and Maktav (2014). Another finding was that the accuracy by triplet images did not significantly improve the results especially against the stereopair with longest base, i.e. 283-284. $\kappa_\lambda = 5.89\ 10^{-12}$ as a Tikhonov regularization coefficient was applied for triplet set in bundle adjustment to solve the ill-conditioned Jacobian matrix (Terlemezoğlu and Topan, 2020). Figure 4 shows the plots of errors after pre and bundle adjustment. Ignoring the local systematic vectors of GCPs, the vectors at ICPs were not systematic as desired. The correlation and validation of EOPs could also be estimated. For instance, an EOP set, i.e. $\underline{P_2} = [X_{s_0}\ Y_{s_0}\ Z_{s_0}]^T$, was chosen as an alternate like in Topan (2022), The correlations were $r_{X_{s_0}Y_{s_0}} = 0.89, r_{X_{s_0}Z_{s_0}} = 0.96$ and $r_{Y_{s_0}Z_{s_0}} = 0.90$ for stereopair 269-283 in triplet case. The correlations for remaining stereopairs were almost similar. All EOPs in each set were reported as invalid, meaning that they can be used with their initial values. As reported by Topan (2022) and Aytekin and Topan (2024), the major limitation was the estimating the look angles of ICPs interpolated from the pre-adjusted look angles of GCPs. This can be overcomed by a proper GCP/ICP distribution following the elimination. In this paper, the results for ICPs in Table 3 were a slightly greater than ±1 GSD since an elimination was not applied. Such kind of limitation was not observed by Topan (2023).

5. Conclusion

This paper presents the Geo3o1 tool developed in the Matlab platform following the author's experience with GeoSpot. Geo3o1 does not aim to develop a new sensor-dependent orientation model, but uses the private models of Pléiades 1A/1B/Neo and SPOT 6/7 and Göktürk 1. The novelty is that the adjustment process is carried out by pre-adjustment and bundle-adjustment. Geo3o1 can be used to evaluate the efficiency of the internal and external orientation parameters. The limitations of Geo3o1 need to be addressed in further studies. Geo3o1 also has the ability to generate orthoimages and digital surface models, which can be added to its options. Researchers can freely access the codes of Geo3o1 through GeoEtrim (2025).

Stereopair	Point	Pre adjustment *(×10⁻⁴ for GCPs)*			Bundle adjustment *(×10⁻² for GCPs)*		
	Type	m_X	m_Y	m_Z	m_X	m_Y	m_Z
283-284	GCP	2.12	0.22	3.76	1.44	0.65	1.72
	ICP	0.63	0.59	0.59	0.63	0.60	0.59
269-283	GCP	3.12	0.31	2.88	1.91	0.88	0.20
	ICP	0.73	0.71	0.78	0.73	0.71	0.78
269-284	GCP	1.34	0.58	0.49	1.09	0.53	1.47
	ICP	1.14	0.64	1.35	1.14	0.65	1.35
Triplet	GCP	2.19	0.21	3.84	1.45	0.68	1.69
	ICP	0.60	0.57	0.62	0.61	0.57	0.61

Table 3. Results of 3D georeferencing accuracy (± meter).

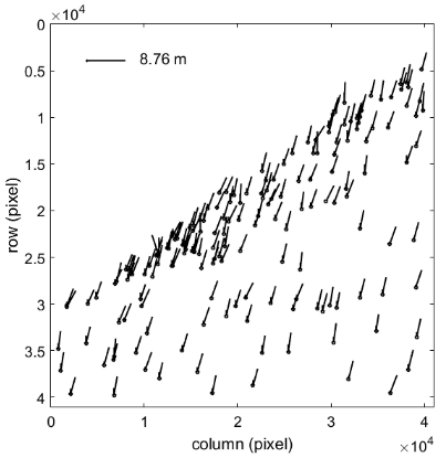

Figure 3. Vector plot of direct georeferencing accurayc for stereopair 283-284.

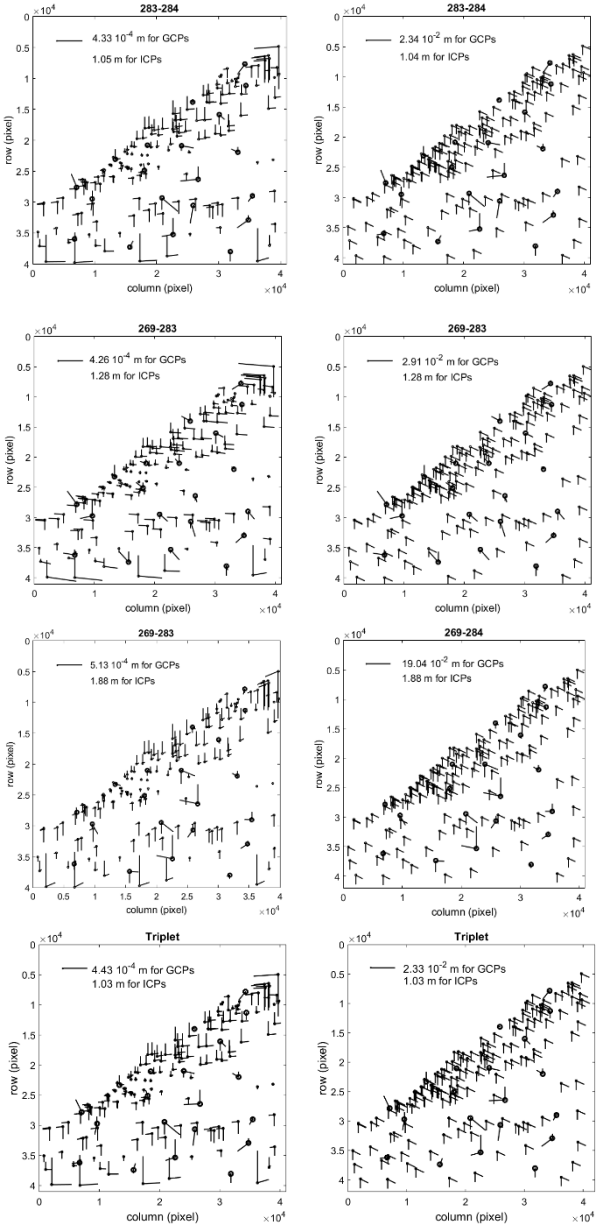

Figure 4. Plot of errors at GCPs (•) and at ICPs (°) after pre (left) and bundle (right) adjustment.

6. Acknowledgements

Thanks are going to Airbus Defense and Space for supporting the images, and to TÜBİTAK (Grant Number: 114Y380) and to Zonguldak Bülent Ecevit University Scientific Research Projects Fund (Grant Number: 2014-47912266-01) for their supporting the projects with field campaign. Specials thanks are also going to Prof. Gürcan Büyüksalih and Dr.-Ing. Karsten Jacobsen for their advising since 2002, to Prof. Derya Maktav for his supervising during the PhD period, Prof. Orhan Kurt, Dr. Mehmet Güven Koçak, Dr. Bilgi Terlemezoğlu, Dr. Gürsu Aytekin, Prof. Fikret Gölgeleyen, and Prof. Bahattin Erdoğan for their scientific contribution and cooperation, and finally to the colleagues in the Department of Geomatics Engineering for the field campaigns.

References

Abdel-Aziz, Y.I., Karara, M., 1971. Direct Linear Transformation from Comparator Co-ordinates into Objectspace Co-ordinates in Close-range Photogrammetry, American Society of Photogrametry Symposium on Close-Range Photogrammetry, pp. 420-475.

Airbus Defence and Space, 2012. Pléiades Imagery User Guide, V 2.0 ed.

Airbus Defence and Space, 2013. SPOT 6 & SPOT 7 Imagery User Guide, SI/DC/13034-v1.0 ed.

Airbus Defence and Space, 2022. Pléiades Neo User Guide, 3 ed.

Aytekin, G., Topan, H., 2024. Unlocking the 3D Georeferencing Accuracy Potential of Göktürk-1 Tri-Stereo Panchromatic Level 2A Images by Sensor-Dependent Orientation Model. Proceedings of the Romanian Academy, Series A 25, 347–358.

Büyüksalih, G., Koçak, G., Topan, H., Oruç, M., Marangoz, A., 2005. SPOT Revisited: Accuracy Assessment, DEM Generation and Validation from Stereo SPOT 5 HRG Images. Photogrammetric Record 20, 130-146.

Fotev, S., Georgiev, N., Nedkov, R., 2005. Viewing Geometry Model Evaluation for Spaceborne Pushbroom Imagery, Proceedings of 2nd International Conference on Recent Advances in Space Technologies 2005, RAST 2005., İstanbul, pp. 540 - 544

GeoEtrim, 2025. GeoEtrim: Geospatial Evaluation and Training of Images, in: Topan, H. (Ed.).

Kapnias, D., Milenov, P., Kay, S., 2008. Guidelines for Best Practice and Quality Checking of Ortho Imagery, European Commission, Joint Research Centre, Institute for the Protection and Security of the Citizen.

Konecny, G., Lohmann, P., Engel, H., Kruck, E., 1987. Evaluation of SPOT imagery on analytical photogrammetric instruments. Photogrammetric Engineering & Remote Sensing 53, 1223-1230.

Leprince, S., Barbot, S., Ayoub, F., Avouac, J.P., 2007. Automatic and precise orthorectification, coregistration, and subpixel correlation of satellite images, application to ground deformation measurements. IEEE Transactions on Geoscience and Remote Sensing 45, 1529-1558.

Leprince, S., Muse, P., Avouac, J.P., 2008. In-flight CCD distortion calibration for pushbroom satellites based on subpixel correlation. IEEE Transactions on Geoscience and Remote Sensing 46, 2675-2683.

OGC, 1999. The OpenGIS® Abstract Specification Topic 6: The Coverage Type and its Subtypes Version 4.

Orun, A.B., 1990. SPOT Satellite Imagery for Topographic Mapping, Department of Civil Engineering, Building and Cartography. Oxford Polytechnic, Oxford.

Orun, A.B., Natarajan, K., 1994. A modified bundle adjustment software for SPOT imagery and photography: Tradeoff. Photogrammetric Engineering and Remote Sensing 60, 1431-1437.

Riazanoff, S., 2004. SPOT 123-4-5 Geometry Handbook, in: Image, S. (Ed.). Spot Image, France.

Terlemezoğlu, B., Topan, H., 2020. Eigenvalue-Based Approaches for Solving an Ill-Posed Problem Arising in Sensor Orientation. IEEE Transactions on Geoscience and Remote Sensing 58, 1920-1930.

Topan, H., 2004. Yörünge Düzeltmeli IRS-1C/1D Pankromatik Mono Görüntüsünün Geometrik Doğruluk ve Bilgi İçeriği Açısından İncelenmesi, Fen Bilimleri Enstitüsü. Zonguldak Karaelmas Üniversitesi.

Topan, H., 2009. Geometric Analysis of High Resolution Space Images Using Parametric Approaches Considering Satellite Orbital Parameters, Department of Geomatics Engineering. Istanbul Technical University, İstanbul, p. 113.

Topan, H., 2022. Geo3o1: A Tool for 3D Georeferencing Accuracy Assessment of Tri-Stereo Images by State-of-the-Art Sensor Dependent Orientation Model. Journal of Applied Remote Sensing 16, 047502.

Topan, H., 2023. First experience of 3D georeferencing accuracy assessment of SPOT 6 stereo panchromatic primary images by sensor-dependent orientation model. Remote Sensing Letters 14, 1294-1302.

Topan, H., Cam, A., Özendi, M., Oruç, M., Jacobsen, K., Taşkanat, T., 2016. Pléiades Project: Assessment of Georeferencing Accuracy, Image Quality, Pansharpening Performence and DSM/DTM Quality, in: L. Halounova, V.Š., C. K. Toth, J. Karas, G. Huadong, N. Haala, A. Habib, P. Reinartz, X. Tang, J. Li, C. Armenakis, G. Grenzdörffer, P. le Roux, S. Stylianidis, R. Blasi, M. Menard, H. Dufourmount, and Z. Li (Ed.), International Archives of Photogrammetry Remote Sensing and Spatial Informaton Sciences. Copernicus Publications, Prague (Czech Republic), pp. 503-510.

Topan, H., Maktav, D., 2014. Efficiency of Orientation Parameters on Georeferencing Accuracy of SPOT-5 HRG Level-1A Stereoimages. IEEE Transactions on Geoscience and Remote Sensing 52, 3683-3694.

Toutin, T., 1983. Analyse Mathématique des Possibilités Cartographiques du Satellite SPOT, d'Études Approfondies, École Nationale des Sciences Géodésiques, Saint-Mandé, France, p. 74.

Weser, T., Rottensteiner, F., Willneff, J., Fraser, C.S., 2007. A Generic Pushbroom Sensor Model For High-Resolution Satellite Imagery Applied to Spot 5, Quickbird and ALOS Data Sets, International Archives of the Photogrammetry, Remote Sensing and Spatial Information Sciences, "High Resolution Earth Imaging for Geospatial Information", Hannover.

Weser, T., Rottensteiner, F., Willneff, J., Poon, J., Fraser, C.S., 2008. Development and Testing of a Generic Sensor Model for Pushbroom Satellite Imagery. The Photogrammetric Record 23, 255-274.